Immune Network
http://dx.doi.org/10.4110/in.2016.16.1.61
pISSN 1598-2629 eISSN 2092-6685
ORIGINAL ARTICLE

TCF4-Targeting miR-124 is Differentially Expressed amongst Dendritic Cell Subsets

Sun Murray Han[1,2#], Hye Young Na[1#], Onju Ham[2,3#], Wanho Choi[1,2], Moah Sohn[1,2], Seul Hye Ryu[1,2], Hyunju In[1,2], Ki-Chul Hwang[3] and Chae Gyu Park[1,2]*

[1]Laboratory of Immunology, [2]Brain Korea 21 PLUS Project for Medical Science, Severance Biomedical Science Institute, Yonsei University College of Medicine, Seoul 03722, [3]Institute for Bio-Medical Convergence, College of Medicine, Catholic Kwandong University, Gangneung 25601, Korea

Dendritic cells (DCs) are professional antigen-presenting cells that sample their environment and present antigens to naïve T lymphocytes for the subsequent antigen-specific immune responses. DCs exist in a range of distinct subpopulations including plasmacytoid DCs (pDCs) and classical DCs (cDCs), with the latter consisting of the cDC1 and cDC2 lineages. Although the roles of DC-specific transcription factors across the DC subsets have become understood, the posttranscriptional mechanisms that regulate DC development are yet to be elucidated. MicroRNAs (miRNAs) are pivotal posttranscriptional regulators of gene expression in a myriad of biological processes, but their contribution to the immune system is just beginning to surface. In this study, our in-house probe collection was screened to identify miRNAs possibly involved in DC development and function by targeting the transcripts of relevant mouse transcription factors. Examination of DC subsets from the culture of mouse bone marrow with Flt3 ligand identified high expression of miR-124 which was able to target the transcript of TCF4, a transcription factor critical for the development and homeostasis of pDCs. Further expression profiling of mouse DC subsets isolated from *in vitro* culture as well as via *ex vivo* purification demonstrated that miR-124 was outstandingly expressed in $CD24^+$ cDC1 cells compared to in pDCs and $CD172\alpha^+$ cDC2 cells. These results imply that miR-124 is likely involved in the processes of DC subset development by posttranscriptional regulation of a transcription factor(s).
[Immune Network 2016;16(1):61-74]

Keywords: Dendritic cells, MicroRNAs, Posttranscriptional Gene Silencing, TCF4

INTRODUCTION

Dendritic cells (DCs) are antigen-presenting cells found in lymphoid as well as non-lymphoid tissues and organs. They principally act as specialized sentinel cells that sample their local environment for antigens, migrate to lymph nodes, and present antigens to naïve T lymphocytes, which is essential for the subsequent antigen-specific T-cell activation and induction of immune responses (1). Many varieties of DCs have been described in both humans and mice with each characterized by particular locations, phenotypic morphologies, and functions. In essence, DCs consist of

Received on November 10, 2015. Revised on January 8, 2016. Accepted on January 15, 2016.

*Corresponding Author. Chae Gyu Park, Laboratory of Immunology, Severance Biomedical Science Institute, Yonsei University College of Medicine, 50-1 Yonsei-ro, Seodaemun-gu, Seoul 03722, Korea. Tel: 82-2-2228-0795; Fax: 82-2-2227-8129; E-mail: ChaeGyu@yuhs.ac
#These authors contributed equally to this work.

Abbreviations: BM, bone marrow; cDCs, classical DCs; CDP, common DC progenitor; CHO cells, Chinese hamster ovary cells; DCs, dendritic cells; EGFP, enhanced green fluorescence protein; Flt3L, Flt3 ligand; IRES, internal ribosomal entry site; Lin, lineage; MCS, multiple cloning site; MDP, macrophage-DC progenitor; miRNA, microRNA; pDCs, plasmacytoid DCs; pri-miRNA, primary miRNA; UTR, untranslated region

a range of functionally distinct subsets that can be identified by their differential expression of particular surface markers (1,2). The DC subsets prevalent in lymphoid tissues include antigen-presenting classical DCs (cDCs) and type 1 interferon-producing plasmacytoid DCs (pDCs). The lymphoid tissue-resident cDCs are further divided into different subtypes including CD8α^+CD24$^+$ cDCs (cDC1), which efficiently cross-present antigens to CD8$^+$ T cells and principally produce IL-12; and CD8α^-CD172α^+ cDCs (cDC2), which present MHC Class II restricted antigens to CD4$^+$ T cells. Also, more DC subtypes develop upon infection or inflammation such as the monocyte-derived inflammatory DCs.

The development of DCs to their respective subset counterparts arise through a multistage process. Like all other immune cells, DCs develop from hematopoietic stem cells in the bone marrow (BM). Hematopoietic stem cells differentiate into the myeloid progenitors, which subsequently differentiate into the macrophage-DC progenitor (MDP) cells and then into the common-DC progenitor (CDP) cells (3). CDPs develop into pre-DCs and then egress from the BM to the periphery, which seed peripheral secondary lymphoid tissues and non-hematopoietic tissues and ultimately mature into either cDCs or pDCs. Development of DC subsets from their progenitor cells can be replicated *in vitro* with various culture conditions. Culture of DC progenitors in BM with the growth factor Flt3 ligand (Flt3L) produces a heterogeneous population containing both cDCs and pDCs, which are equivalent to their in situ counterparts with respect to cell surface marker expression, transcription factor reliance, cytokine production, receptor molecule expression, and antigen-presenting ability to T cells (4,5). Principally, DC subsets originated from Flt3L-cultured BM cells correspond to those of steady-state cDC populations. Beyond these mature DC subsets, relevant progenitor and precursor populations can also be identified and isolated from BM cells in steady state as well in culture with Flt3L (6,7).

In light of these investigatory advances, the roles of transcription factors in DC development and their dynamic profiles across the subsets have become well understood (8-10). For example, the transcription factor PU.1 has been described to play a role in the development of all DCs. Meanwhile, STAT5 is known to drive the development of cDCs over pDCs through the inhibition of transcription factor interferon regulatory factor 8 (Irf8), whereas immunoglobin transcription factor 2 (TCF4) is known to drive pDC development over cDCs by directly activating Irf8 and other pro-pDC transcription factors such as SpiB (9-11). As such, a comprehensive group of transcription factors and their involvement in the particular stages of DC development have been mapped. In contrast to these transcriptional mechanisms, posttranscriptional mechanisms that regulate DC development are less well understood. With the heterogeneity of subsets and wide-ranging function of DCs, the natural question arises on how DC differentiation and development is regulated besides the orchestration of growth factors and transcription factors. Recently, increasing evidence has shown that microRNAs (miRNAs) play an important role in fine-tuning DC development and function.

miRNAs are an evolutionarily conserved class of short, endogenous, non-coding RNAs about 19～23 nucleotides long that regulate protein synthesis by targeting the complementary 3' untranslated region (UTR) of mRNAs for translational repression and degradation (12). miRNA biogenesis begins with the transcription of a miRNA gene to generate a primary miRNA (pri-miRNA) transcript, which is ultimately processed into a mature 19～23 bp miRNA and incorporated into an RNA-induced silencing complex (13) for the translational repression or degradation of target mRNAs. A key characteristic of miRNAs is that each has the ability to inhibit a myriad of mRNAs, and each mRNA can be targeted by many miRNAs. This is suggestive of a complex network of miRNAs surrounding DC development.

miRNAs have been shown to be vital in controlling many processes within the immune system. Their involvement in regulating T- and B-lymphocyte development has been established of late and their wide-ranging roles in cell differentiation, homeostasis, cytokine responses, and interactions with pathogens and tolerance induction among others have been described (14). More recent progressions have attempted to describe the role of miRNAs in DC development (15). Several miRNAs have been specifically attributed to the direct regulation of certain DC functions. More have been identified by the comprehensive mapping of dynamic miRNA profiles across the subsets and tested to confirm their necessity in DC lineage commitment (15-21). In the present study, to identify miRNAs possibly involved in DC development and function, we screened for the expression of candidate miRNAs that target the 3'UTR

of relevant transcriptional factors using our in-house probe collection. Our screening results indicated that miR-124, able to target the 3'UTR of TCF4 transcript, was highly detected in mouse DC subsets. Further expression profiling of mouse DC subsets demonstrated that miR-124 was outstandingly expressed in $CD24^+$ cDC1 cells compared to in pDCs and $CD172\alpha^+$ cDC2 cells. Our findings imply that miR-124 is likely involved in the processes of DC subset development by posttranscriptional regulation of a transcription factor(s).

MATERIALS AND METHODS

Animals

Mice were maintained and bred in specific pathogen-free facilities of the Department of Laboratory Animal Resources at the Yonsei University College of Medicine. C57BL/6 mice were purchased from Jackson Laboratory (Bar Harbor, ME, USA) and Orient Bio (Seongnam, Republic of Korea). Animal care and experiments were conducted according to the guidelines and protocols approved by the Institutional Animal Care and Use Committee (IACUC) of Yonsei University College of Medicine. Only healthy male mice at 6 to 12 weeks of age were used throughout this study.

Cells, antibodies, and reagents

Chinese hamster ovary (CHO) cells (CHO-S cells; Gibco, Life Technologies, Carlsbad, CA, USA) were cultured in DMC7 medium composed of DMEM containing L-glutamine, high glucose, and pyruvate (HyClone, Logan, UT, USA) and 7% fetal calf serum (FCS; HyClone) supplemented with 1× solutions of non-essential amino acids and antibiotic-antimycotic (HyClone). The following conjugated antibodies were purchased from BioLegend (San Diego, CA, USA): APC-Cy™7-conjugated anti-I-A/I-E, anti-CD11c, anti-B220/CD45R, anti-CD45, anti-Rat IgG2b κ Isotype Control; Alexa Fluor® 647-conjugated anti-CD117; APC-conjugated anti-B220/ CD45R, anti-PDCA-1 (BST2, CD317), anti-CD135; PE- Cy™7-conjugated anti-Ly6G, anti-CD3, anti-CD11c, anti-CD19, anti-Ter119, anti-DX5, anti-I-A/I-E, anti-NK1.1, anti-Gr-1, anti-Sca-1; PerCP-Cy™5.5- conjugated anti-Ly6C, anti-CD11c, anti-CD24, anti-CD117, anti-CD172α (Sirpα); PE-conjugated anti-SiglecH, anti-CD11c, anti-CD115, anti-CD117, anti-CD135, anti-Armenian Hamster (AH) IgG Isotype Control; FITC-conjugated anti-CD172α; Alexa Fluor® 488-conjugated anti-Ly6C, anti-CD172α, anti- PDCA-1, anti-CD24, anti-CD45.2; Brilliant Violet™ 421 (BV421)-conjugated anti-CD11c, anti-CD45.1, anti-CD45.2, anti-CD115, anti-AH IgG Isotype Control; biotin-conjugated anti-NK1.1, anti-DX5, anti Ter119, anti-Ly6G, anti-CD3, anti-CD19, anti-CD135. LIVE/DEAD® fixable dead cell stain kit (Life Technologies) and propidium iodide (Roche, Indianapolis, IN, USA) were purchased and used according to the manufacturers' instructions.

Production of mouse Flt3L from CHO cells

The cDNA of mouse Flt3L was cloned by RT-PCR of total splenic RNA from C57BL/6 mice, and was used to generate a construct encoding **s**oluble **F**LAG and **O**LLAS tagged **Flt3L**, internal ribosomal entry site (**IRES**), and enhanced green fluorescence protein (**EGFP**), i.e., SFO.Flt3L-IRES-EGFP. The GenBank accession number for the sequence including the extracellular domain of mouse Flt3L is GU168042, and the IRES-EGFP sequence is from pIRES-EGFP plasmid (Clontech, Mountain View, CA, USA). CHO cells were then transfected using Lipofectamine 2000 (Life Technologies), with a mammalian expression vector plasmid encoding SFO.Flt3L-IRES-EGFP under CMV promoter and a neomycin resistance gene, constructed with the backbone of pEGFP-N1 (Clontech). CHO/Flt3L cells stably expressing the SFO.Flt3L-IRES-EGFP were produced by the following steps: (i) treatment of transfected CHO cells with G418 (1.5 mg/ml) for 1 week; (ii) enrichment of EGFP-positive CHO cells with FACSAria II cell sorter (BD Biosciences, San Diego, CA, USA); (iii) generation of clonal cells by limiting dilutions of FACS-sorted EGFP- high CHO/Flt3L cells; and (iv) selection of CHO/Flt3L clones after evaluating both levels of EGFP expression by FACS analysis and Flt3L secretion by anti-OLLAS Western blot analysis (22). Chosen CHO/Flt3L cells were cultured in cell culture flasks with DMC7 to produce CHO/ Flt3L-conditioned medium.

Western blot analysis

Different amounts of supernatant from CHO/Flt3L cell culture were mixed with an equal volume of 2×SDS PAGE sample buffer and boiled at 95°C for 5 min. The samples were then separated in 12% SDS-PAGE and transferred onto PVDF membranes (Thermo Fisher Scientific, Rockford, IL, USA) before being incubated with anti-OLLAS monoclonal antibody (22). Anti-OLLAS antibody-reactive

bands on the blots were examined after incubation with peroxidase-conjugated anti-rat IgG antibody (Southern-Biotech, Birmingham, AL, USA) and subsequent visualization with SuperSignal™ West Pico Chemiluminescent Substrate (Thermo Fisher Scientific) and ImageQuant™ LAS 4000 mini (GE Healthcare Life Sciences, Pittsburgh, PA, USA). Graded quantities (0～160 ng) of purified OLLAS-tagged Gag p41 protein (2) were evaluated in parallel for quantification of OLLAS-tagged Flt3L bands.

Preparation and culture of primary cells

Mice were sacrificed by asphyxiation in a CO_2 chamber. Whole splenocyte suspension was prepared by cutting and mincing extracted spleens followed by grinding with frosted glasses and cell strainers (BD Biosciences). Whole BM cell suspension was prepared by flushing out femurs and tibias excised from the hind legs of mice in sterile conditions as described previously (23). Then, the single cell suspension was cultured in either 48- or 24-well tissue culture plates at 1×10^6 or 2×10^6 cells per well, respectively, with DMC7 containing different doses of Flt3L, i.e., CHO/Flt3L conditioned medium described above. During the culture, half of the medium in each well was carefully removed and replenished with fresh DMC7 containing Flt3L every 2 days until harvest for use in subsequent experiments.

Flow cytometry

Single cell suspensions from the harvest of mouse organ tissues or cultures thereof were incubated with 2.4G2 (Fc blocker) hybridoma supernatant and washed with FACS buffer (2% FCS, 2 mM EDTA, 0.1% sodium azide). Then, each sample was incubated with the appropriate mixture of fluorochrome-conjugated monoclonal antibodies and live/dead staining dye for 30 min at 4°C and washed twice with FACS buffer. The samples were then analyzed with FACSVerse flow cytometer (BD Biosciences) or sorting with FACSAria II cell sorter (BD Biosciences). As for sorting, the isolated cells with 90% or higher purity were utilized for subsequent experiments. Gating criteria for respective precursor and DC populations were as follows. With the lineage (Lin) markers of CD3, CD19, Ly6G, NK1.1, DX5, Ter119: for pDCs, $Lin^-CD11c^+B220^+$ $PDCA\text{-}1^+SiglecH^+$; for cDC1, $Lin^-CD11c^+MHCII^+B220^-$ $CD24^{high}CD172\alpha^-$; for cDC2, $Lin^-CD11c^+MHCII^+B220^-$ $CD24^{int}CD172\alpha^+$. With the lineage markers of CD3, CD19, Ly6G, NK1.1, DX5, Ter119, MHCII, B220: for MDP, $Lin^-CD11c^-CD115^+CD135^+CD117^{high}$; for CDP, $Lin^-CD11c^-CD115^+CD135^+CD117^{int}$. Flow cytometric data were analyzed using FlowJo software (FlowJo, Ashland, OR, USA).

Isolation of RNA

Total RNA was isolated from sorted cells from cultured or uncultured mouse primary cells using TRIzol® Reagent (Life Technologies) following the manufacturer's instructions.

Real-time RT-PCR of miRNA

For miRNA expression profiling, 100 ng of purified total RNA was used for reverse transcription using Taqman® MicroRNA Reverse Transcriptase Kit (Applied Biosystems, Foster City, CA, USA). The resultant cDNA was used in combination with Taqman® MicroRNA Assays (Applied Biosystems) for respective miRNA and U6 control transcripts and Taqman® Universal Master Mix II (Applied Biosystems) for PCR according to the manufacturer's instructions. The amplification and detection of products were performed in a Light Cycler 480 II (Roche) with an initial denaturation at 95°C for 10 min, followed by 40～60 cycles of amplification at 95°C for 15 sec and 60°C for 60 sec, before cooling. The threshold cycle (Ct) of miR-124 expression was automatically defined, located in the linear amplification phase of the PCR, and normalized to the control U6 (ΔCt value). The relative difference in expression levels of miR-124 in the sorted cells ($\Delta\Delta$Ct) was calculated and presented as the fold induction ($2^{-\Delta\Delta Ct}$).

Real-time RT-PCR of transcription factors and pri-miR-124

For pri-miR-124 profiling, 100 ng of purified total RNA was used for reverse transcription using PrimeScript™ RT Reagent Kit (TaKaRa Bio Inc., Ohtsu, Japan). The resultant cDNA was used in combination with primer oligonucleotides designed for DC-related transcription factors (5) and pri-mmu-miR-124-1/-2/-3 (24) and SYBR® Premix Ex Taq II (TaKaRa) for PCR according to the manufacturer's instructions. Sequences for the primer oligonucleotides, synthesized by Cosmo Genetech (Seoul, Korea), are as follows: TCF4, 5'-TGAGATCAAATCCGACGA-3' forward, 5'-CGTTATTGCTAGATCTTGACCT-3' reverse; Batf3, 5'-AGACCCAGAAGGCTGACAA-3' forward, 5'-CTGCACAAAGTTCATAGGACAC-3' reverse; Irf8, 5'-

AAGGGCGTGTTCGTGAAG-3' forward, 5'-GGTGGCG TAGAATTGCTG-3' reverse; pri-miR-124-1, 5'-GCCTCT CTCTCCGTGT-3' forward, 5'-CCATTCTTGGCATTCA-3' reverse; pri-miR-124-2, 5'-AGAGACTCTGCTCTCCG TGT-3' forward, 5'-CTCCGCTCTTGGCATTC-3' reverse; pri-miR-124-3, 5'-GGCTGCGTGTTCACAG-3' forward, 5'-ATCCCGCGTGCCTTA-3' reverse; GAPDH, 5'-ACA GTCCATGCCATCACTGCC-3' forward, 5'-GCCTGCTT CACCACCTTCTTG-3' reverse. The amplification and detection of products were performed in a Light Cycler 480 II (Roche) with an initial denaturation at 95°C for 5 min, followed by 40～60 cycles of PCR at 95°C for 5 sec and 50°C for 30 sec, before melting and cooling. The relative difference in expression levels for pri-miR-124-1/-2/-3 in the sorted cells was calculated and presented as described above but with normalization to the control GAPDH.

Luciferase activity assay

The predicted target genes of miR-124 were identified using a public database (miRWalk2.0, http://www.umm.uni-heidelberg.de/apps/zmf/mirwalk). Sections containing the miR-124 binding site of the 3'UTR of TCF4 and Zbtb46 were cloned into pmirGLO Dual-Luciferase miRNA Target Expression Vector (Promega, Fitchburg, WI, USA) independently. HeLa cells were seeded at 2.5×10^4 cells per well in a 24-well plate. After 48 hrs, the pmirGLO vector containing the target mRNA binding site for the miR-124 was co-transfected with mmu-miR-124 mimic (Applied Biosystems) or the negative control using Lipofectamine 2000 (Life Technologies). Luciferase activity was measured after 48 hrs using Dual Luciferase Assay System (Promega) according to the manufacturer's instructions on a luminometer (Promega). Renilla luciferase activity was used to normalize the transfection efficiency. Each assay was repeated at least 3 times.

Statistical analysis

Experiments with multiplicated samples were presented as mean±SEM from at least three independent experiments. Statistical comparisons between different groups were analyzed using unpaired Student's t-test using SigmaPlot (Systat Software, San Jose, CA). Statistical significance is denoted by the p values equal or below 0.05 (*), 0.01 (**), and 0.001 (***). Data were plotted for graphs with SigmaPlot.

RESULTS

Production of Flt3L and culture of bone marrow

We generated the extracellular domain sequence of mouse Flt3L fused with the sequences of signal peptide, FLAG tag, and OLLAS tag. This soluble FLAG and OLLAS tagged Flt3L (SFO.Flt3L) sequence was devised to express with IRES and EGFP under CMV promoter (Fig. 1A) following transfection into CHO cells. CHO cells expressing high levels of Flt3L were enriched by sorting for EGFP, cloned, and named CHO/Flt3L cells (Fig. 1B). The conditioned medium from CHO/Flt3L cells was produced in large volume, sterilized by filtration, and blotted with anti-OLLAS antibody for the determination of Flt3L concentration before being added into the culture of BM cells. According to the anti-OLLAS Western blot analysis, the CHO/Flt3L conditioned medium was evaluated to contain approximately 10 μg/ml of Flt3L (Fig. 1C). To verify the efficacy of Flt3L produced, graded doses of CHO/Flt3L conditioned medium were used to culture BM for the generation of DCs *in vitro*. Higher concentrations of Flt3L in BM culture induced DC differentiation more efficiently (Fig. 1D). Especially, when the culture media were composed of 10% or higher amount of the Flt3L conditioned medium (up to 50%), the increase in number of DCs in BM culture became conspicuous (data not shown for BM cultures in media with 25% or 50% of the Flt3L conditioned medium). As estimated by Western blot analysis above, 10% content of the Flt3L conditioned medium corresponds to 1 μg/ml of Flt3L in culture medium. The efficacy to induce DCs *in vivo* by this Flt3L protein has also been demonstrated previously (25,26).

Candidate miRNAs with potential to regulate DC development

To identify miRNAs possibly involved in DC development, a Web-based miRNA-target interaction database miRWalk2.0 (27), which amalgamates data from a collection of miRNA-target prediction programs, was used. Ten gene targets that are prominent transcription factors known to have a pivotal role in DC development − TCF4, Bcl6, Irf2, Irf4, Irf8, Id2, SpiB, Batf3, Notch2, Zbtb46 − were picked for the prediction software to identify miRNAs that possibly regulate these genes by binding to their 3'UTR. From the provided list of miRNAs that have a high potential to bind to the 3'UTR of these transcription factors,

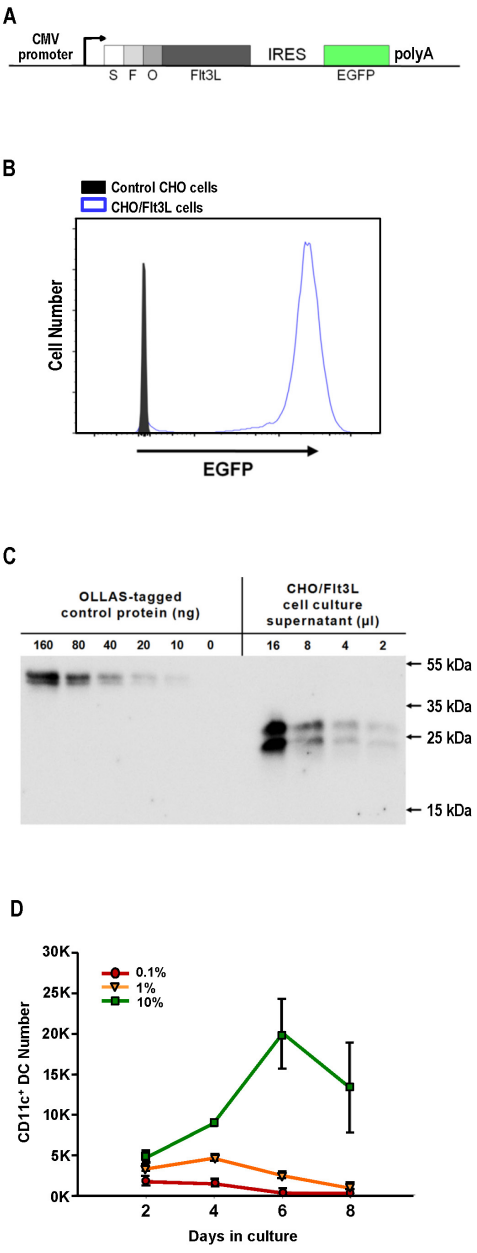

Figure 1. Culture of BM cells with CHO/Flt3L-conditioned medium produces DCs *in vitro*. (A) Diagram for the expression construct that encodes soluble FLAG and OLLAS tagged mouse Flt3L gene with IRES and EGFP (SFO.Flt3L-IRES-EGFP). (B) CHO cells stably transfected with SFO.Flt3L-IRES-EGFP (CHO/Flt3L cells) were selected and cloned for the high expression of EGFP. (C) Concentration of mouse Flt3L protein in the supernatant from CHO/Flt3L cell culture was titrated using anti-OLLAS monoclonal antibody. (D) Time-course quantification of $CD11c^+$ DCs per well for each culture condition containing 0.1～10% of Flt3L conditioned medium.

candidate miRNAs were selected dependent upon availability of detection reagents in our in-house miRNA probe collection. Overall, 20 candidate miRNAs were specified according to the analyses of 3'UTR sequences from the 10 transcription factors (Supplemental Fig. 1).

Screening of candidate miRNA expression in DCs from BM cultured with Flt3L

In preliminary efforts to reveal miRNAs that may play a role in DC development, expression profiles of the candidate miRNAs were assessed in Flt3L culture system of mouse BM cells. Using our in-house probe collection, the expressions of 20 candidate miRNAs were screened in $CD11c^+$ DCs derived from BM culture with Flt3L, which were further assorted into $B220^-$ cDCs and $B220^+$ pDCs (Fig. 2A). Total RNAs isolated from these two subsets of cultured DCs were subjected to analysis of miRNA expression profile by real-time RT-PCR. When the expression of candidate miRNAs was normalized and their relative levels were compared, an exceedingly high expression of miR-124 was observed in the $B220^-$ cDC population from BM culture with Flt3L (Fig. 2B). In the case of each individual candidate miRNA profile, all were expressed more in $B220^-$ cDCs than in $B220^+$ pDCs except for miR-17 (Fig. 2C). Exceptionally high expression of miR-124 in cDCs and its contrasting expression between cDCs and pDCs in BM-derived DCs cultured with Flt3L suggest that miR-124 may also be differentially expressed during ontogeny of DCs *in vivo* and may play a role in their development.

Direct regulation of transcript containing 3'UTR of TCF4 by miR-124

According to the analysis of miRNA-target interactions above, miR-124 is predicted to bind to the 3'UTR of TCF4 (Supplemental Fig. 1A). miR-124 is also expected to bind to Zbtb46 although the probability is low (i.e., the sum of prediction algorithms with significant scores is 1; Supplemental Fig. 1J). To see whether miR-124 actually binds to these genes and regulates their expression, a dual luciferase reporter assay was performed using a pmirGLO vector (Fig. 3A). A section, 342 bps, of the 3'UTR of TCF4 containing the predicted binding site of miR-124 was inserted into the multiple cloning site (MCS) of a pmirGLO vector (Fig. 3B). A 480 bp section of the 3'UTR of Zbtb46 was cloned likewise into a pmirGLO vector (Fig. 3C). The

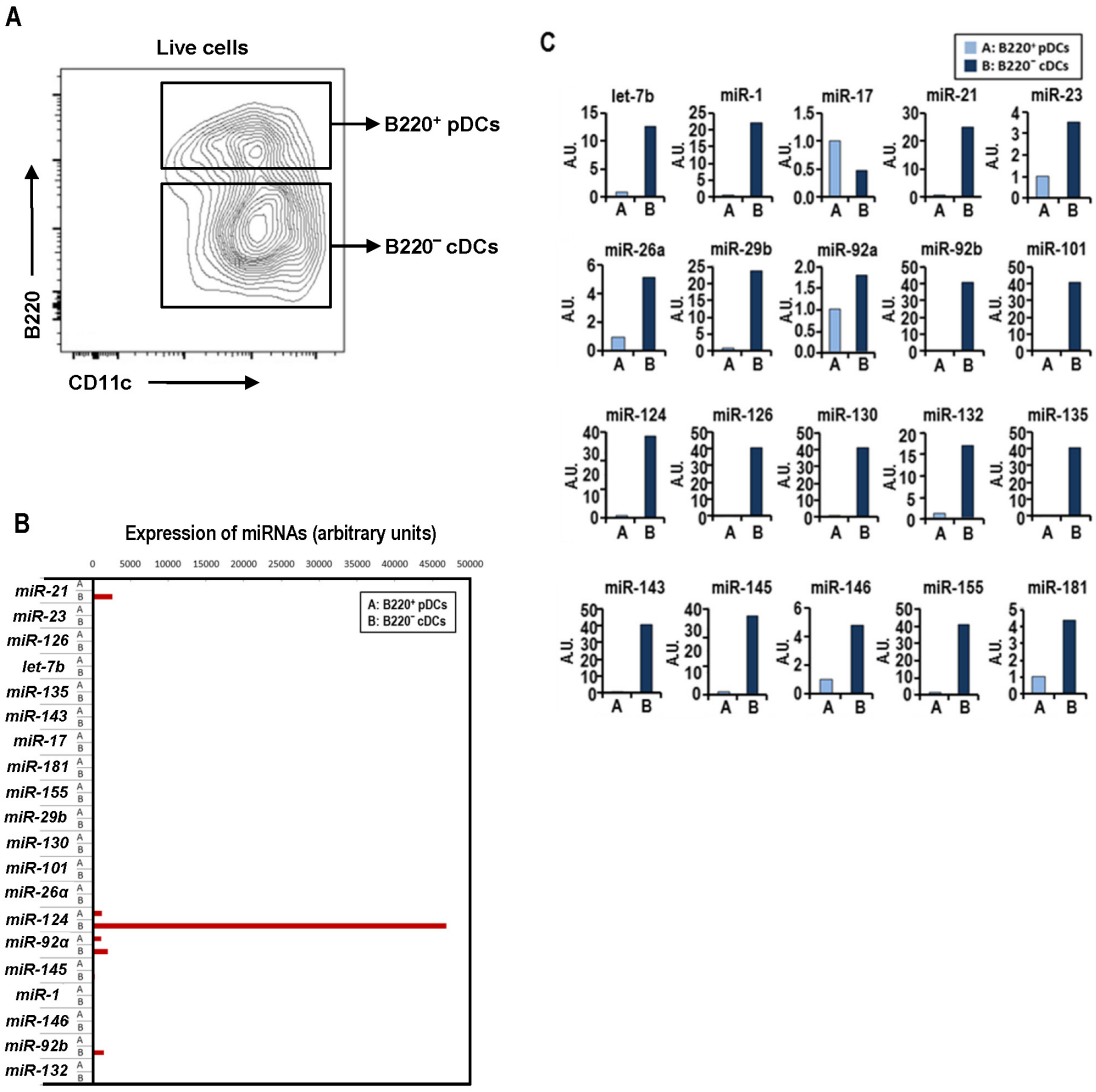

Figure 2. Preliminary expression profiles of candidate miRNAs in Flt3L-cultured DC subsets. (A) Gating strategies for pDCs and cDCs present in BM culture with Flt3L for 8 days. (B) Normalized expression levels of candidate miRNAs in DC subsets isolated from BM culture with Flt3L. (C) Relative expression of individual candidate miRNAs between pDCs and cDCs isolated from BM culture with Flt3L.

cloned vectors were co-transfected with miR-124 mimic or the negative control into HeLa cells and the luciferase activity was measured. The assay showed that the overexpression of miR-124 was able to down-regulate luciferase activity of the pmirGLO-TCF4 vector by ~30% while not those of the pmirGLO-control or pmirGLO-Zbtb46 (Fig. 3D). Besides, the sequences of miR-124 binding site found in 3'UTRs of both mouse and human TCF4 transcripts are highly conserved (Fig. 3E). Therefore, it appears that miR-124 might directly bind to both 3'UTRs of mouse and human TCF4 and thus posttranscriptionally regulate their activity.

Higher expression of miR-124 in cDC1 cells from BM culture with Flt3L

TCF4 is a critical transcription factor in the development

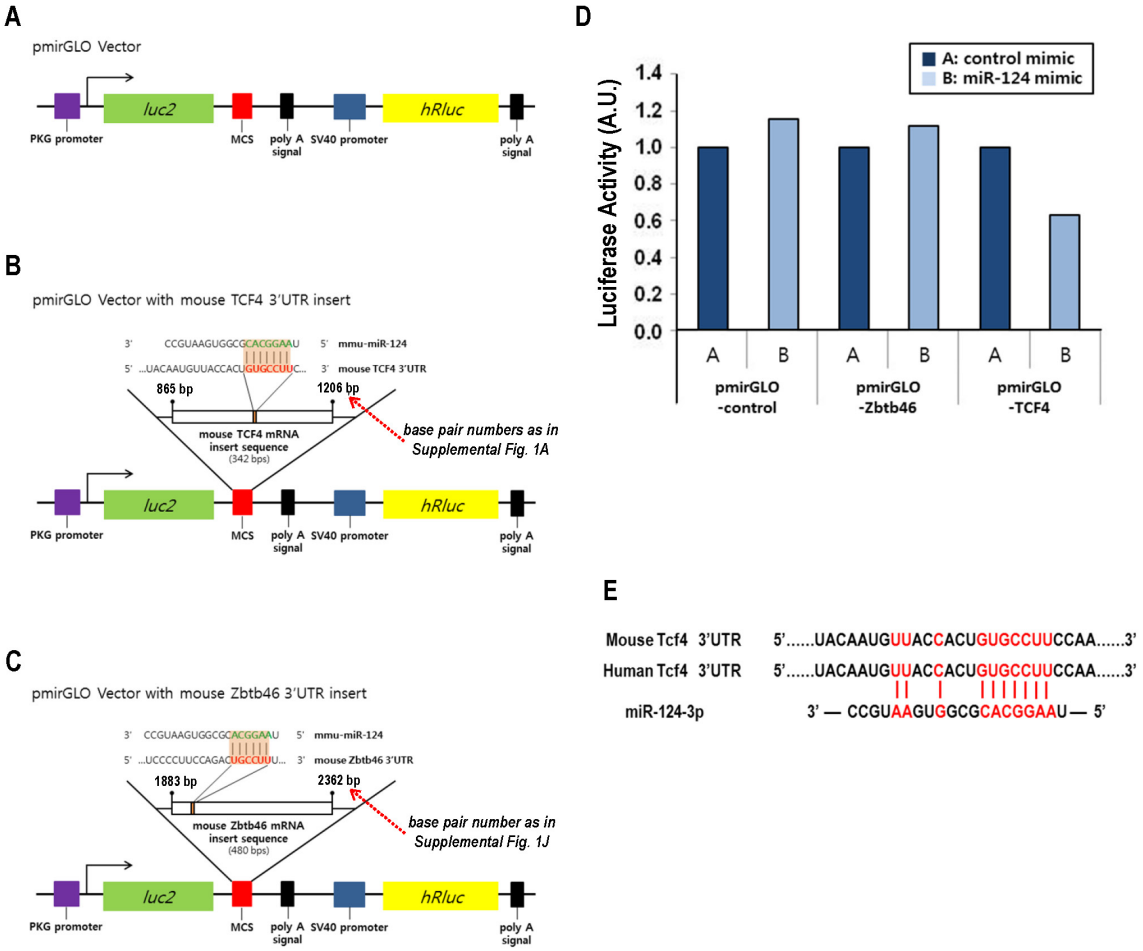

Figure 3. Regulation of gene expression by miR-124 via direct binding to 3'UTR of target transcript. Diagrams of the luciferase reporter vector pmirGLO constructs encoding (A) no insert, i.e., control, or 3'UTR from (B) TCF4 and (C) Zbtb46. (D) Histogram of normalized luciferase activities obtained from HeLa cells co-transfected with the respective reporter constructs and miR-124 mimic or negative control. Representative results are shown from 3 independent experiments. (E) Predicted binding site of miR-124 in the 3'UTRs of mouse and human TCF4.

and homeostasis of pDCs and is expressed at higher levels in pDCs and pDC precursors than in other DCs and progenitors (5,28). Therefore, it seems developmentally relevant that lower expression of miR-124 in pDCs than in cDCs was observed amongst BM-derived DCs cultured with Flt3L in our preliminary screening (Fig. 2). As previously demonstrated by others (7,29,30), we were able to culture BM cells *in vitro* with Flt3L for 6 to 12 days to efficiently produce three major DC subsets that respectively correspond to pDC, cDC1, and cDC2 lineage cells in lymphoid tissues *in vivo*. These DC populations from Flt3L-cultured BM were identified and isolated as per their surface markers of $CD11c^{+}B220^{+}$ for pDCs, $CD11c^{+}B220^{-}CD24^{+}CD172\alpha^{-}$ for cDC1, and $CD11c^{+}B220^{-}CD172\alpha^{+}CD24^{int}$ for cDC2 (Fig. 4A). Then, these three DC populations purified from BM culture with Flt3L by flow cytometric sorting were subjected to RNA extraction and real-time RT-PCR. As mentioned above, the dynamic and differential expression of various transcription factors across the DC subsets is critical for DC development (10). Expressions of TCF4, Batf3, and Irf8 in the DC subsets isolated from BM culture with Flt3L (Fig. 4B) were parallel to those previously reported in the DC subsets isolated from lymphoid tissues (9), indicating that the isolated DC

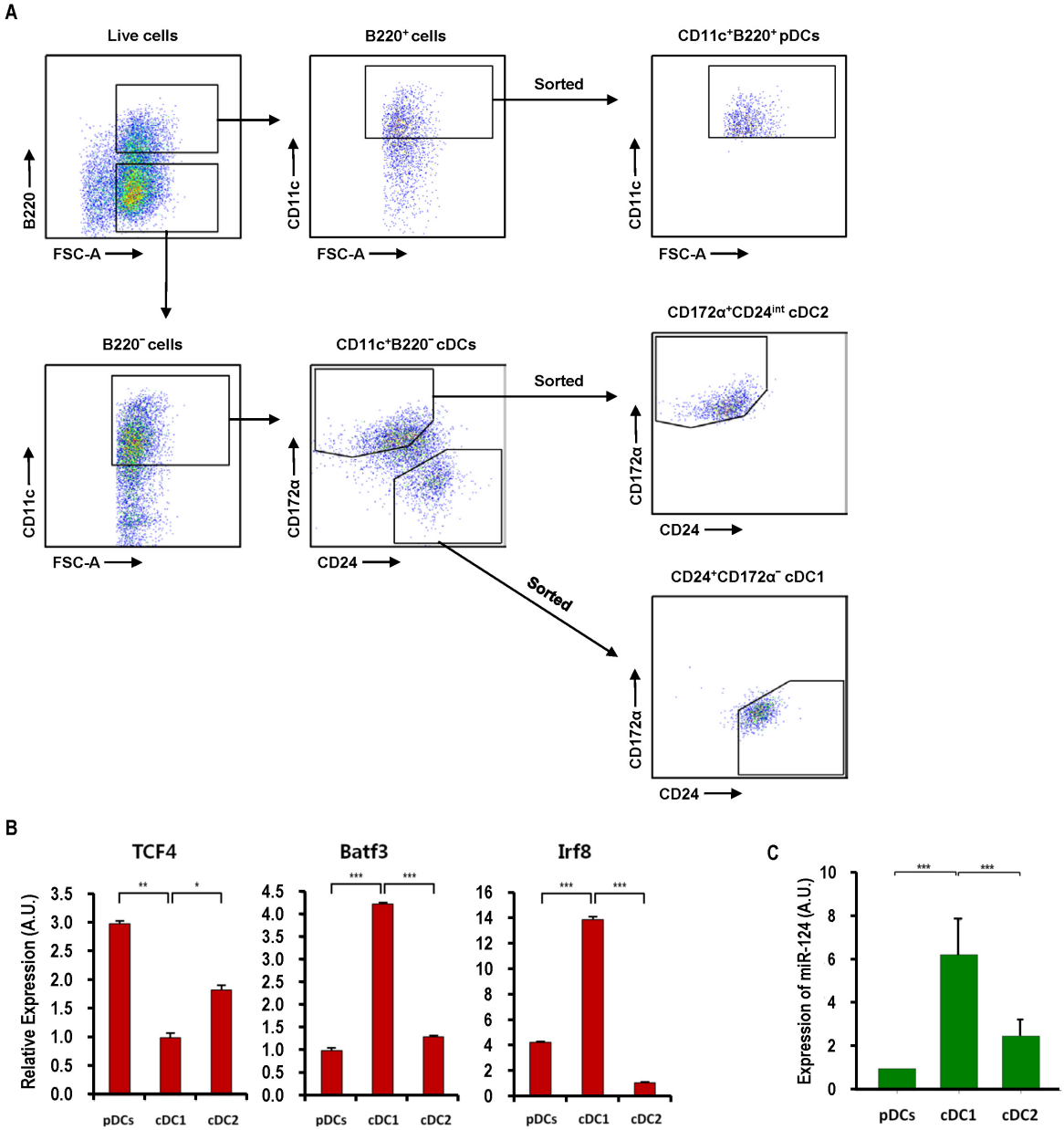

Figure 4. High expression of miR-124 in cDC1 cells from BM culture with Flt3L. (A) Gating and sorting strategies for pDC, cDC1, and cDC2 cells from BM culture with Flt3L. (B) Relative expression of 3 transcription factors critical to DC development is determined amongst different DC subsets by real-time RT-PCR. Representative results are shown from 2 independent experiments. (C) Relative expression of miR-124 is assessed amongst different DC subsets by real-time RT-PCR. Data from 3 independent experiments are presented in histogram. Error bars indicate mean±SEM across all samples from 3 independent experiments. *p≤0.05; **p≤0.01; ***p≤0.001.

subsets were classified appropriately. Expression of miR-124, similar to the results of the preliminary screen (Fig. 2), was lower in pDCs than in cDCs, i.e., cDC1 and cDC2 cells (Fig. 4C). Moreover, cDC1 cells were shown to express significantly higher levels of miR-124 than both pDCs and cDC2 cells.

Expression of miR-124 is higher in cDC1 cells than in other DCs, DC precursors, and progenitors in BM and spleen

To further verify the expression profiles of miR-124 amongst DC subsets present in BM culture with Flt3L, we examined the expression of miR-124 from DC subsets and progenitors present in steady-state BM. MDP, CDP, pDC, cDC1, and cDC2 cells present in mouse BM were respectively purified *ex vivo* by flow cytometric sorting according to their surface makers (Fig. 5A-C). When the extracted RNAs of the respective DC subsets and progenitors isolated from BM were analyzed by real-time RT-PCR and compared, miR-124 expression was prominently found in cDC1 cells at a level much higher than those of MDP, CDP, and other DC subsets (Fig. 5D). In addition, we also had several BM populations of pre-DCs, including pre-cDCs and pre-pDCs (6,7,31), purified and analyzed for their expressions of miR-124, which were lower than that of cDC1 cells but similar to those of other DC subsets and progenitors (data not shown). Therefore, higher expression of miR-124 is consistently found in the cDC1 lineage from both BM cells and BM-derived cell cultures with Flt3L. Then, to observe the patterns of miR-124 expression in steady-state spleen, DC subsets and pre-DCs were sorted *ex vivo* from freshly prepared splenocytes according to their surface makers (Fig. 6A-C). Real-time RT-PCR of the extracted RNA from the sorted splenic cells also revealed a relatively high expression of miR-124 in cDC1 cells compared to other DC subsets and pre-DCs in spleen (Fig. 6D), therefore suggesting that the abundant expression of miR-124 might be important to the development of all cDC1 lineage cells in general.

All three miR-124 precursor transcripts contribute to miR-124 expression in cDC1 cells

As depicted in Fig. 7A, there are three primary miRNA genes for miR-124: pri-miR-124-1, pri-miR-124-2, and pri-miR-124-3 (32,33). Three transcripts originate from these three different genes on separate chromosomes but all convert into the same mature miR-124 sequence. With

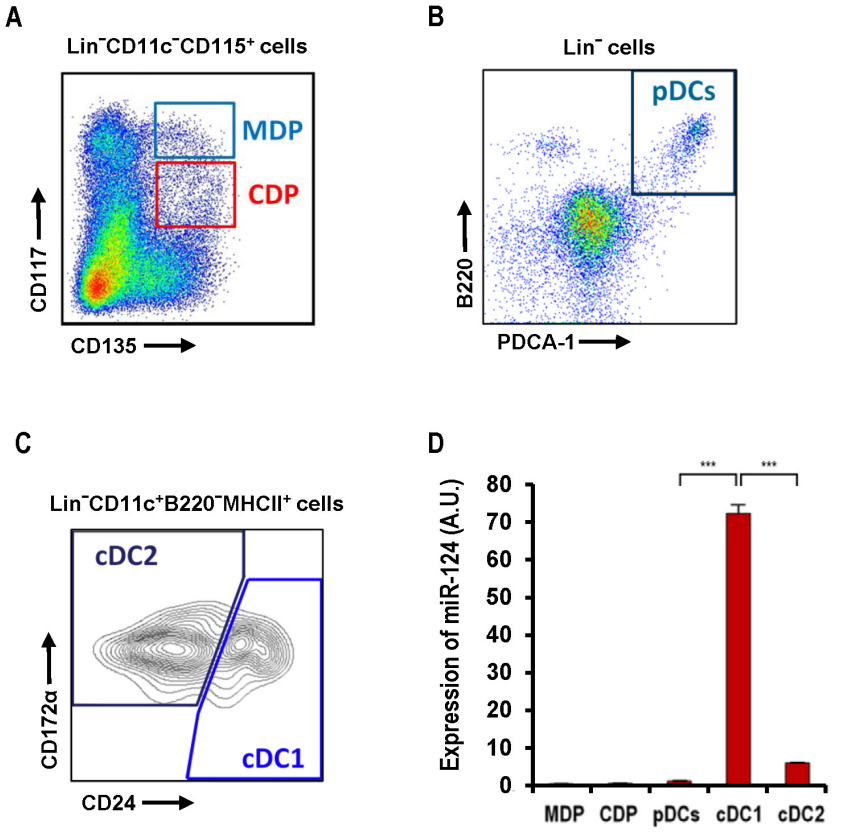

Figure 5. Prominent expression of miR-124 in cDC1 cells in BM. Gating strategies for (A) MDP, CDP, (B) pDC, (C) cDC1, and cDC2 cells in BM. (D) Relative expression of miR-124 is assessed amongst different progenitors and DC subsets by real-time RT-PCR. Representative results are shown from 3 independent experiments. ***$p \leq 0.001$.

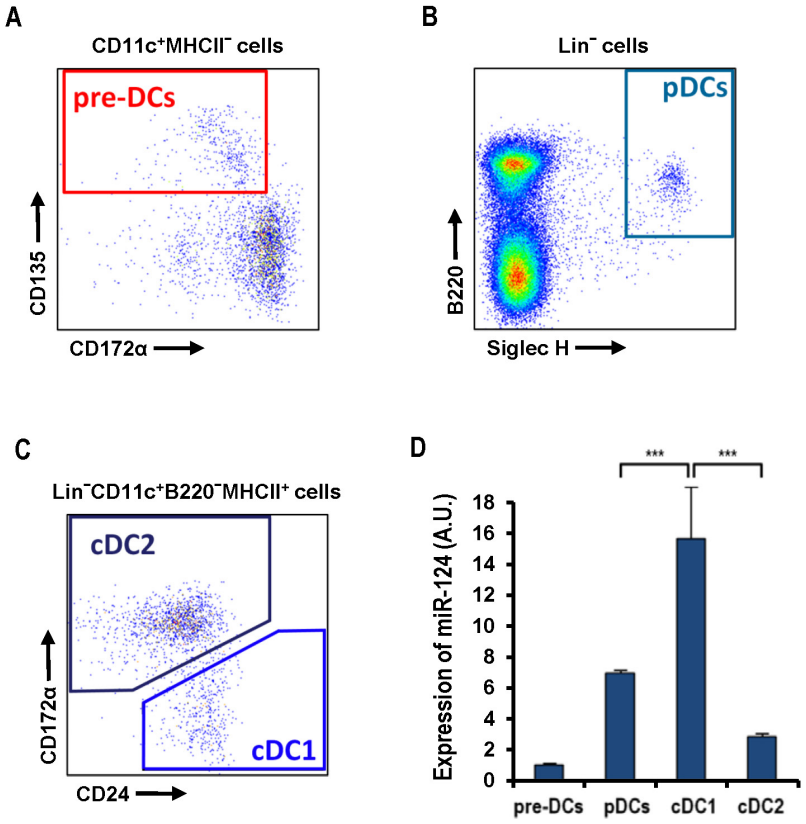

Figure 6. Elevated expression of miR-124 in cDC1 cells in spleen. Gating strategies for (A) pre-DC, (B) pDC, (C) cDC1, and cDC2 cells in spleen. (D) Relative expression of miR-124 is evaluated amongst different DC precursor and subsets by real-time RT-PCR. Representative results are shown from 3 independent experiments. ***$p \leq 0.001$.

oligonucleotide probes to distinguish and detect the three pri-miR-124 transcripts (24), real-time RT-PCR was performed to determine which miR-124 precursors were expressed more in the cDC1 lineage. Expression profiling of pri-miR-124 in the cDC1 cells from steady-state BM (Fig. 7B) and spleen (Fig. 7C) showed similar patterns of miR-124 precursor expression. In both tissues, cDC1 cells showed that pri-miR-124-1 was expressed the least and pri-miR-124-3 was expressed the most but all three precursors were expressed within the ranges of no significant statistical difference. In addition, expression of the three pri-miR-124 genes was measured in other DC subsets where transcripts of all three precursor genes were also detected significantly (data not shown). In other words, the definitive expression of all three pri-miR-124 transcripts indicates that they all contribute significantly to the generation of mature miR-124 in cDC1 lineage cells.

DISCUSSION

MicroRNA-124 is known as the most abundant microRNA expressed in neuronal cells (34,35). Although many miRNAs are starting to be linked to immunological processes, miR-124 remains unmentioned. Therefore, our finding of the outstanding and differential expression of miR-124 in BM-derived DCs cultured with Flt3L is intriguing as they are paralleled with DC development *in vivo*. Since homeostasis of DCs *in vivo* is critically dependent on Flt3L, we aimed to critically define the dynamic profile of miR-124 in the DC subpopulations and delineate its interplay with relevant transcription factors that influence the development and function of particular DC subsets. Analyzing the prediction algorithm software, TCF4 was shown to be a probable target of miR-124 while Zbtb46 was shown to be a less likely target. Although it would be important to show the levels of TCF4 or Zbtb46 proteins following treatment with miR-124 mimic in naturally TCF4- or Zbtb46-expressing cells, we could not carry out those experiments in such cells as pDCs and

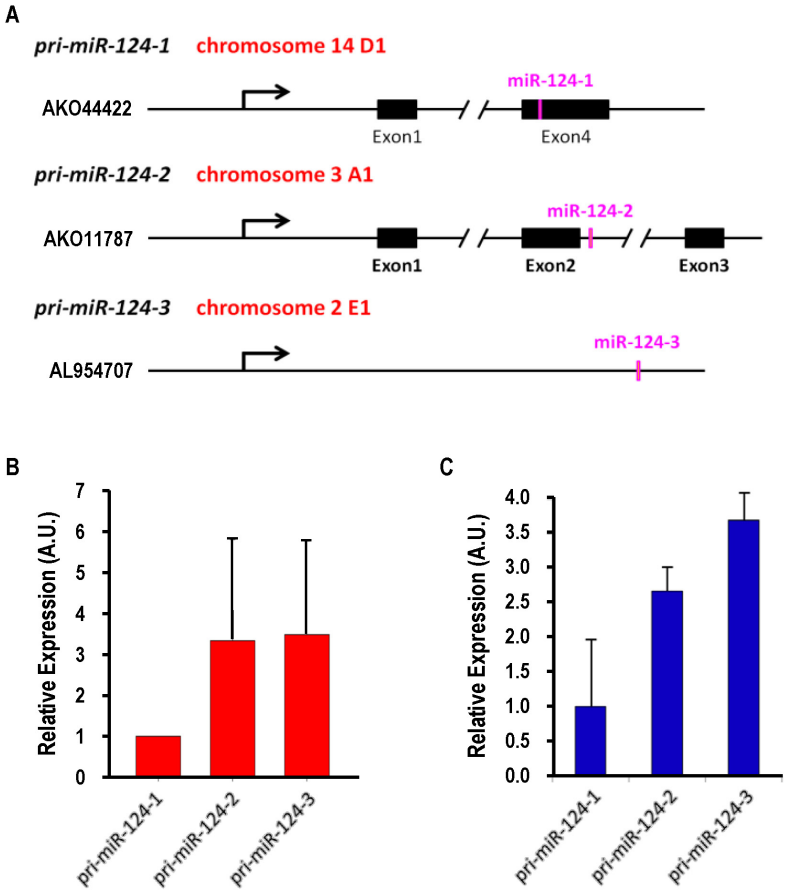

Figure 7. All three primary miR-124 genes are actively transcribed in DCs. (A) Genomic map of three pri-miR-124 genes on three different chromosomal locations are illustrated with their sequence information of GenBank accession numbers. (B) Relative expression of three pri-miR-124 genes is determined from cDC1 cells in BM by real-time RT-PCR. Results combined from 2 independent experiments are shown. (C) Relative expression of three pri-miR-124 genes is assessed from cDC1 cells in spleen by real-time RT-PCR.

pre-DCs but performed dual luciferase assays in HeLa cells instead. Symmetrical to the prediction software, the luciferase activity assay showed that miR-124 mimic can bind and regulate the transcript carrying a 3'UTR section of TCF4.

Since TCF4 has been established to be a critical gene in the development and homeostasis of pDCs, this data suggested that miR-124 may play a role in this process. This led us to hypothesize that miR-124 would be least expressed in pDCs, as its high expression would more effectively target TCF4 mRNA for degradation and thus inhibit pDC development and function. The miR-124 expression profiles of Flt3L-cultured DC subsets correlated with this hypothesis so that miR-124 was least expressed in the pDC subset. Further expression profiling in steady-state BM and spleen, however, showed that miR-124 expression was conspicuously higher only in the cDC1 lineage but lower in both pDCs and cDC2 cells as well as in precursors and progenitors. This hints that miR-124, like most other miRNAs, does not act on DC development one-dimensionally through single miRNA to single target/transcription factor mechanism, but instead acts through single miRNA to multiple targets/transcription factors mechanism. Therefore, we speculate that the differential expression of miR-124 in different subsets may influence DC development broadly and profoundly.

Vital role of several miRNAs in development of specific DC subsets has been characterized in the mice genetically deficient of such miRNA genes (16,19). Unlike those miRNAs, miR-124 has three precursor genes. Moreover, all three pri-miR-124 genes located on different chromosomes appear to significantly contribute to the expression of mature miR-124 in DC subsets. It would be quite difficult and unlikely that the triple knockout mice deficient of all three pri-miR-124 genes become available in the near future. Therefore, it is not currently possible to dem-

onstrate the *in vivo* role of miR-124. Although the effect is transient and limited, transfection of its mimicking or inhibiting molecules into DC precursors and progenitors followed by culture with Flt3L will be able to validate the role of miR-124. All in all, the dynamic profiles of miR-124 expression are consistent within the in vitro-generated DC subsets and their in situ counterparts in lymphoid tissues. Highly dynamic activity of miR-124 during DC development requires elucidation of its purpose for such fluctuation.

ACKNOWLEDGEMENTS

We thank Young Hee Nam for her help with flow cytometry at the Flow Cytometry Core of the Yonsei Biomedical Research Institute in the Yonsei University College of Medicine. We were supported by grants from the National Research Foundation of Korea (NRF-2013R1A1A2058427, NRF-2014R1A4A1008625) and a faculty research grant of Yonsei University College of Medicine for 2014 (6-2014-0062) to CGP, and the Brain Korea 21 PLUS Project for Medical Science, Yonsei University.

CONFLICTS OF INTEREST

The authors have no financial conflict of interest.

REFERENCES

1. Steinman, R. M. 2012. Decisions about dendritic cells: past, present, and future. *Annu. Rev. Immunol.* 30: 1-22.
2. Park, C. G. 2014. Vaccine strategies utilizing C-type lectin receptors on dendritic cells *in vivo*. *Clin. Exp. Vaccine Res.* 3: 149-154.
3. Steinman, R. M., and J. Idoyaga. 2010. Features of the dendritic cell lineage. *Immunol. Rev.* 234: 5-17.
4. Kingston, D., M. A. Schmid, N. Onai, A. Obata-Onai, D. Baumjohann, and M. G. Manz. 2009. The concerted action of GM-CSF and Flt3-ligand on *in vivo* dendritic cell homeostasis. *Blood* 114: 835-843.
5. Onai, N., K. Kurabayashi, M. Hosoi-Amaike, N. Toyama-Sorimachi, K. Matsushima, K. Inaba, and T. Ohteki. 2013. A clonogenic progenitor with prominent plasmacytoid dendritic cell developmental potential. *Immunity* 38: 943-957.
6. Grajales-Reyes, G. E., A. Iwata, J. Albring, X. Wu, R. Tussiwand, W. Kc, N. M. Kretzer, C. G. Briseno, V. Durai, P. Bagadia, M. Haldar, J. Schonheit, F. Rosenbauer, T. L. Murphy, and K. M. Murphy. 2015. Batf3 maintains autoactivation of Irf8 for commitment of a CD8alpha(+) conventional DC clonogenic progenitor. *Nat. Immunol.* 16: 708-717.
7. Schlitzer, A., V. Sivakamasundari, J. Chen, H. R. Sumatoh, J. Schreuder, J. Lum, B. Malleret, S. Zhang, A. Larbi, F. Zolezzi, L. Renia, M. Poidinger, S. Naik, E. W. Newell, P. Robson, and F. Ginhoux. 2015. Identification of cDC1- and cDC2-committed DC progenitors reveals early lineage priming at the common DC progenitor stage in the bone marrow. *Nat. Immunol.* 16: 718-728.
8. Geissmann, F., M. G. Manz, S. Jung, M. H. Sieweke, M. Merad, and K. Ley. 2010. Development of monocytes, macrophages, and dendritic cells. *Science* 327: 656-661.
9. Satpathy, A. T., X. Wu, J. C. Albring, and K. M. Murphy. 2012. Re(de)fining the dendritic cell lineage. *Nat. Immunol.* 13: 1145-1154.
10. Murphy, K. M. 2013. Transcriptional control of dendritic cell development. *Adv. Immunol.* 120: 239-267.
11. Esashi, E., Y. H. Wang, O. Perng, X. F. Qin, Y. J. Liu, and S. S. Watowich. 2008. The signal transducer STAT5 inhibits plasmacytoid dendritic cell development by suppressing transcription factor IRF8. *Immunity* 28: 509-520.
12. Li, Z., and T. M. Rana. 2014. Therapeutic targeting of microRNAs: current status and future challenges. *Nat. Rev. Drug Discov.* 13: 622-638.
13. Ha, M., and V. N. Kim. 2014. Regulation of microRNA biogenesis. *Nat. Rev. Mol. Cell Biol.* 15: 509-524.
14. Johanson, T. M., J. P. Skinner, A. Kumar, Y. Zhan, A. M. Lew, and M. M. Chong. 2014. The role of microRNAs in lymphopoiesis. *Int. J .Hematol.* 100: 246-253.
15. Smyth, L. A., D. A. Boardman, S. L. Tung, R. Lechler, and G. Lombardi. 2015. MicroRNAs affect dendritic cell function and phenotype. *Immunology* 144: 197-205.
16. Mildner, A., E. Chapnik, O. Manor, S. Yona, K. W. Kim, T. Aychek, D. Varol, G. Beck, Z. B. Itzhaki, E. Feldmesser, I. Amit, E. Hornstein, and S. Jung. 2013. Mononuclear phagocyte miRNome analysis identifies miR-142 as critical regulator of murine dendritic cell homeostasis. *Blood* 121: 1016-1027.
17. Karrich, J. J., L. C. Jachimowski, M. Libouban, A. Iyer, K. Brandwijk, E. W. Taanman-Kueter, M. Nagasawa, E. C. de Jong, C. H. Uittenbogaart, and B. Blom. 2013. MicroRNA-146a regulates survival and maturation of human plasmacytoid dendritic cells. *Blood* 122: 3001-3009.
18. Su, X., C. Qian, Q. Zhang, J. Hou, Y. Gu, Y. Han, Y. Chen, M. Jiang, and X. Cao. 2013. miRNomes of haematopoietic stem cells and dendritic cells identify miR-30b as a regulator of Notch1. *Nat. Commun.* 4: 2903.
19. Agudo, J., A. Ruzo, N. Tung, H. Salmon, M. Leboeuf, D. Hashimoto, C. Becker, L. A. Garrett-Sinha, A. Baccarini, M. Merad, and B. D. Brown. 2014. The miR-126-VEGFR2 axis controls the innate response to pathogen-associated nucleic acids. *Nat. Immunol.* 15: 54-62.
20. Park, H., X. Huang, C. Lu, M. S. Cairo, and X. Zhou. 2015. MicroRNA-146a and microRNA-146b regulate human dendritic cell apoptosis and cytokine production by targeting TRAF6 and IRAK1 proteins. *J. Biol. Chem.* 290: 2831-2841.
21. Johanson, T. M., M. Cmero, J. Wettenhall, A. M. Lew, Y. Zhan, and M. M. Chong. 2015. A microRNA expression atlas of mouse dendritic cell development. *Immunol. Cell Biol.* 93: 480-485.
22. Park, S. H., C. Cheong, J. Idoyaga, J. Y. Kim, J. H. Choi, Y. Do, H. Lee, J. H. Jo, Y. S. Oh, W. Im, R. M. Steinman, and C.

G. Park. 2008. Generation and application of new rat monoclonal antibodies against synthetic FLAG and OLLAS tags for improved immunodetection. *J. Immunol. Methods* 331: 27-38.
23. Inaba, K., W. J. Swiggard, R. M. Steinman, N. Romani, G. Schuler, and C. Brinster. 2009. Isolation of dendritic cells. *Curr. Protoc. Immunol.* Chapter 3: Unit 3.7
24. Real, F. M., R. Sekido, D. G. Lupianez, R. Lovell-Badge, R. Jimenez, and M. Burgos. 2013. A microRNA (mmu-miR-124) prevents Sox9 expression in developing mouse ovarian cells. *Biol. Reprod.* 89: 78.
25. Darrasse-Jeze, G., S. Deroubaix, H. Mouquet, G. D. Victora, T. Eisenreich, K. H. Yao, R. F. Masilamani, M. L. Dustin, A. Rudensky, K. Liu, and M. C. Nussenzweig. 2009. Feedback control of regulatory T cell homeostasis by dendritic cells *in vivo*. *J. Exp. Med.* 206: 1853-1862.
26. Choi, J. H., C. Cheong, D. B. Dandamudi, C. G. Park, A. Rodriguez, S. Mehandru, K. Velinzon, I. H. Jung, J. Y. Yoo, G. T. Oh, and R. M. Steinman. 2011. Flt3 signaling-dependent dendritic cells protect against atherosclerosis. *Immunity* 35: 819-831.
27. Dweep, H., and N. Gretz. 2015. miRWalk2.0: a comprehensive atlas of microRNA-target interactions. *Nat. Methods* 12: 697.
28. Cisse, B., M. L. Caton, M. Lehner, T. Maeda, S. Scheu, R. Locksley, D. Holmberg, C. Zweier, N. S. den Hollander, S. G. Kant, W. Holter, A. Rauch, Y. Zhuang, and B. Reizis. 2008. Transcription factor E2-2 is an essential and specific regulator of plasmacytoid dendritic cell development. *Cell* 135: 37-48.
29. Naik, S. H., A. I. Proietto, N. S. Wilson, A. Dakic, P. Schnorrer, M. Fuchsberger, M. H. Lahoud, M. O'Keeffe, Q. X. Shao, W. F. Chen, J. A. Villadangos, K. Shortman, and L. Wu. 2005. Cutting edge: generation of splenic $CD8^+$ and $CD8^-$ dendritic cell equivalents in Fms-like tyrosine kinase 3 ligand bone marrow cultures. *J. Immunol.* 174: 6592-6597.
30. Naik, S. H., P. Sathe, H. Y. Park, D. Metcalf, A. I. Proietto, A. Dakic, S. Carotta, M. O'Keeffe, M. Bahlo, A. Papenfuss, J. Y. Kwak, L. Wu, and K. Shortman. 2007. Development of plasmacytoid and conventional dendritic cell subtypes from single precursor cells derived *in vitro* and *in vivo*. *Nat. Immunol.* 8: 1217-1226.
31. Liu, K., G. D. Victora, T. A. Schwickert, P. Guermonprez, M. M. Meredith, K. Yao, F. F. Chu, G. J. Randolph, A. Y. Rudensky, and M. Nussenzweig. 2009. *In vivo* analysis of dendritic cell development and homeostasis. *Science* 324: 392-397.
32. Kozomara, A., and S. Griffiths-Jones. 2014. miRBase: annotating high confidence microRNAs using deep sequencing data. *Nucleic Acids Res.* 42: D68-D73.
33. Qiu, S., Y. Feng, G. LeSage, Y. Zhang, C. Stuart, L. He, Y. Li, Y. Caudle, Y. Peng, and D. Yin. 2015. Chronic morphine-induced microRNA-124 promotes microglial immunosuppression by modulating P65 and TRAF6. *J. Immunol.* 194: 1021-1030.
34. Baudet, M. L., K. H. Zivraj, C. breu-Goodger, A. Muldal, J. Armisen, C. Blenkiron, L. D. Goldstein, E. A. Miska, and C. E. Holt. 2012. miR-124 acts through CoREST to control onset of Sema3A sensitivity in navigating retinal growth cones. *Nat. Neurosci.* 15: 29-38.
35. Sonntag, K. C., T. U. Woo, and A. M. Krichevsky. 2012. Converging miRNA functions in diverse brain disorders: a case for miR-124 and miR-126. *Exp. Neurol.* 235: 427-435.

Supplemental Figure 1

A

Mouse TCF4 - 3'UTR

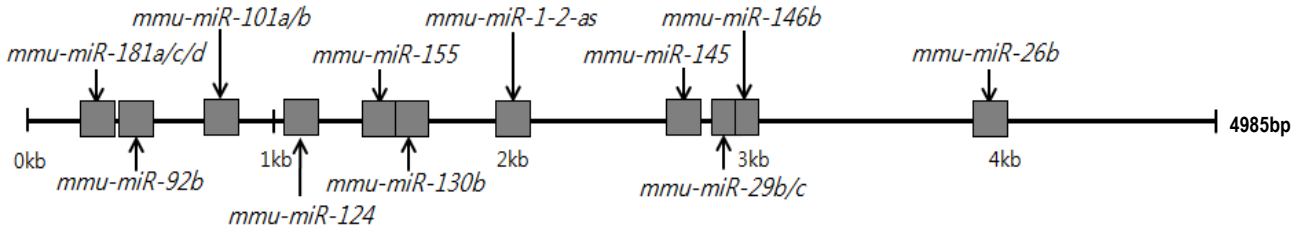

Gene	MicroRNA	StemLoop ID	Sequence (5' → 3')	miRDB	miRWalk	miRanda	Targetscan	SUM
Tcf4	mmu-miR-155	mmu-mir-155	UUAAUGCUAAUUGUGAUAGGGGU	1	1	1	1	4
Tcf4	mmu-miR-29b	mmu-mir-29b-2	CUGGUUUCACAUGGUGGCUUAGAUU	0	1	1	1	3
Tcf4	mmu-miR-101a	mmu-mir-101a	UACAGUACUGUGAUAACUGAA	0	1	1	1	3
Tcf4	mmu-miR-26b	mmu-mir-26b	UUCAAGUAAUUCAGGAUAGGU	0	1	1	1	3
Tcf4	mmu-miR-181d	mmu-mir-181d	AACAUUCAUUGUUGUCGGUGGGU	0	1	1	1	3
Tcf4	mmu-miR-130b	mmu-mir-130b	CAGUGCAAUGAUGAAAGGGCAU	0	1	1	1	3
Tcf4	mmu-miR-181c	mmu-mir-181c	AACAUUCAACCUGUCGGUGAGU	0	1	1	1	3
Tcf4	mmu-miR-29c	mmu-mir-29c	UAGCACCAUUUGAAAUCGGUUA	0	1	1	1	3
Tcf4	mmu-miR-181a	mmu-mir-181a-1	AACAUUCAACGCUGUCGGUGAGU	0	1	1	1	3
Tcf4	mmu-miR-124	mmu-mir-124-2	UAAGGCACGCGGUGAAUGCC	0	1	1	1	3
Tcf4	mmu-miR-92b	mmu-mir-92b	UAUUGCACUCGUCCCGGCCUCC	0	1	1	1	3
Tcf4	mmu-miR-145	mmu-mir-145	GUCCAGUUUUCCCAGGAAUCCCU	0	1	1	1	3
Tcf4	mmu-miR-1-2-as	mmu-mir-1-2-as	UACAUACUUCUUUACAUUCCA	0	1	1	1	3
Tcf4	mmu-miR-101b	mmu-mir-101b	GUACAGUACUGUGAUAGCU	0	1	1	1	3
Tcf4	mmu-miR-146b	mmu-mir-146b	UGAGAACUGAAUUCCAUAGGCU	0	1	1	1	3

PITA and RNA22 omitted because TCF4 not registered.
Only binding sites of miRNA with SUM ≥ 3 shown.

B

Mouse Bcl6 - 3'UTR

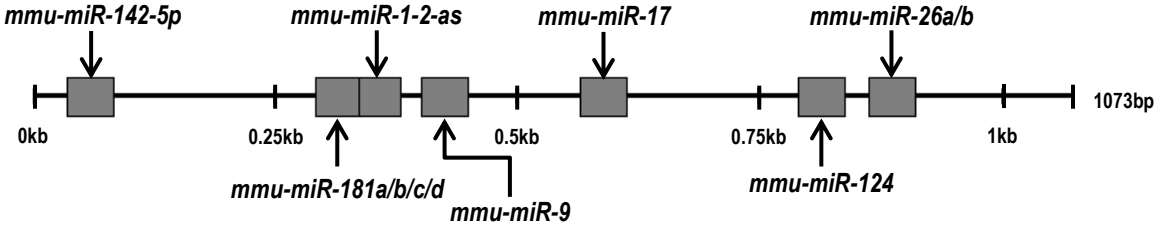

Gene	MicroRNA	StemLoop ID	Sequence (5' → 3')	miRanda	miRDB	miRWalk	PITA	RNA22	Targetscan	SUM
Bcl6	mmu-miR-9	mmu-mir-9-1	UCUUUGGUUAUCUAGCUGUAUGA	1	1	1	1	1	1	6
Bcl6	mmu-miR-17	mmu-mir-17	CAAAGUGCUUACAGUGCAGGUAG	0	0	1	1	1	1	4
Bcl6	mmu-miR-181a	mmu-mir-181a-1	AACAUUCAACGCUGUCGGUGAGU	0	0	1	1	1	1	4
Bcl6	mmu-miR-181b	mmu-mir-181b-1	AACAUUCAUUGCUGUCGGUGGGU	0	0	1	1	1	1	4
Bcl6	mmu-miR-181c	mmu-mir-181c	AACAUUCAACCUGUCGGUGAGU	0	0	1	1	1	1	4
Bcl6	mmu-miR-181d	mmu-mir-181d	AACAUUCAUUGUUGUCGGUGGGU	0	0	1	1	1	1	4
Bcl6	mmu-miR-26a	mmu-mir-26a-1	UUCAAGUAAUCCAGGAUAGGCU	0	0	1	1	1	1	4
Bcl6	mmu-miR-124	mmu-mir-124-1	UAAGGCACGCGGUGAAUGCC	1	0	1	1	0	1	4
Bcl6	mmu-miR-142-5p	mmu-mir-142	CAUAAAGUAGAAAGCACUACU	1	0	1	1	0	1	4
Bcl6	mmu-miR-1-2-as	mmu-mir-1-2-as	UACAUACUUCUUUACAUUCCA	0	0	1	1	0	1	3
Bcl6	mmu-miR-26b	mmu-mir-26b	UUCAAGUAAUUCAGGAUAGGU	0	0	1	1	0	1	3

Only binding sites of miRNA with SUM ≥ 3 shown.

Supplemental Figure 1

C

Mouse Irf2 - 3'UTR

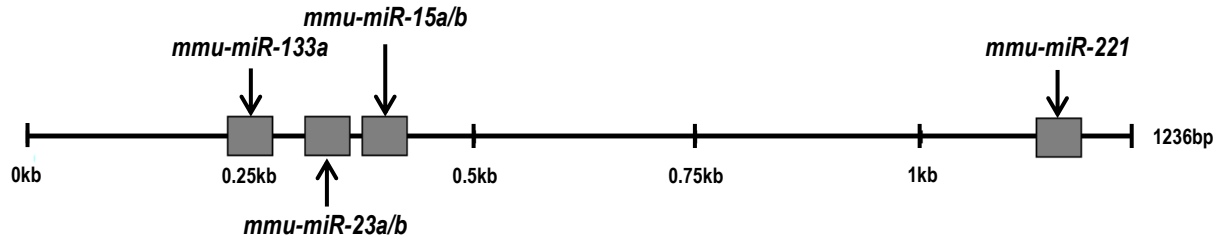

Gene	MicroRNA	StemLoop ID	Sequence (5′ → 3′)	miRWalk	miRanda	miRDB	PITA	RNA22	Targetscan	SUM
Irf2	mmu-miR-23a	mmu-mir-23a	AUCACAUUGCCAGGGAUUUCC	1	1	1	1	0	1	5
Irf2	mmu-miR-23b	mmu-mir-23b	AUCACAUUGCCAGGGAUUACC	1	1	1	1	0	1	5
Irf2	mmu-miR-221	mmu-mir-221	AGCUACAUUGUCUGCUGGGUUUC	1	1	1	1	0	1	5
Irf2	mmu-miR-133a	mmu-mir-133a-2	UUUGGUCCCCUUCAACCAGCUG	1	1	0	1	0	1	4
Irf2	mmu-miR-15a	mmu-miR-15a	UAGCAGCACAUAAUGGUUUGUG	1	0	0	1	1	0	3
Irf2	mmu-miR-15b	mmu-miR-15b	UAGCAGCACAUCAUGGUUUACA	1	0	0	1	1	0	3

Only binding sites of miRNA with SUM ≥ 3 shown

D

Mouse Irf4 - 3'UTR

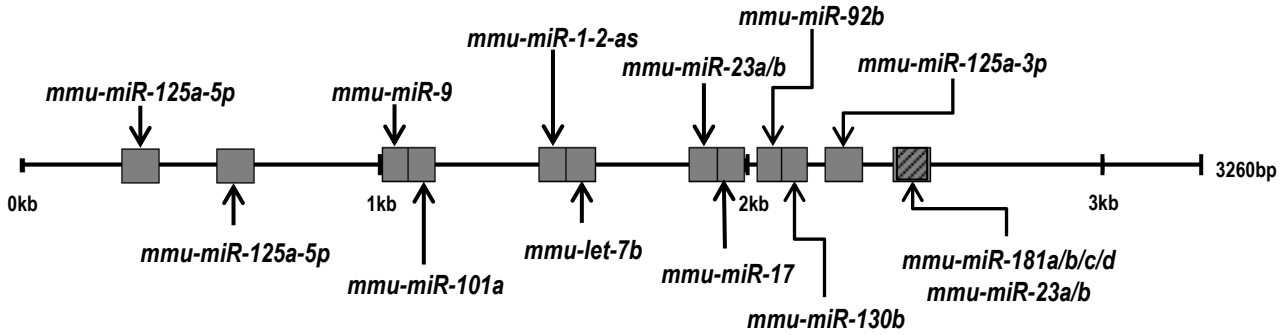

Gene	MicroRNA	StemLoop ID	Sequence (5′ → 3′)	miRWalk	miRanda	miRDB	PITA	RNA22	Targetscan	SUM
Irf4	mmu-miR-125a-5p	mmu-mir-125a	UCCCUGAGACCCUUUAACCUGUGA	1	1	1	1	1	1	6
Irf4	mmu-miR-181c	mmu-mir-181c	AACAUUCAACCUGUCGGUGAGU	1	1	0	1	1	1	5
Irf4	mmu-miR-1-2-as	mmu-mir-1-2-as	UACAUACUUCUUUACAUUCCA	1	1	1	0	1	1	5
Irf4	mmu-miR-181d	mmu-mir-181d	AACAUUCAUUGUUGUCGGUGGGU	1	1	0	1	1	1	5
Irf4	mmu-miR-23a	mmu-mir-23a	AUCACAUUGCCAGGGAUUUCC	1	1	0	1	1	1	5
Irf4	mmu-miR-92b	mmu-mir-92b	UAUUGCACUCGUCCCGGCCUCC	1	1	0	1	1	1	5
Irf4	mmu-miR-23b	mmu-mir-23b	AUCACAUUGCCAGGGAUUACC	1	1	0	1	1	1	5
Irf4	mmu-miR-181a	mmu-mir-181a-1	AACAUUCAACGCUGUCGGUGAGU	1	1	0	1	1	1	5
Irf4	mmu-miR-130b	mmu-mir-130b	CAGUGCAAUGAUGAAAGGGCAU	1	1	0	1	1	1	5
Irf4	mmu-miR-181b	mmu-mir-181b-1	AACAUUCAUUGCUGUCGGUGGGU	1	1	0	1	1	1	5
Irf4	mmu-miR-17	mmu-mir-17	CAAAGUGCUUACAGUGCAGGUAG	1	0	0	1	1	1	4
Irf4	mmu-miR-101a	mmu-mir-101a	UACAGUACUGUGAUAACUGAA	1	1	0	0	1	1	4
Irf4	mmu-let-7b	mmu-let-7b	UGAGGUAGUAGGUUGUGUGGUU	1	0	0	1	1	1	4
Irf4	mmu-miR-9	mmu-mir-9-1	UCUUUGGUUAUCUAGCUGUAUGA	1	0	0	1	1	1	4
Irf4	mmu-miR-146a	mmu-mir-146a	UGAGAACUGAAUUCCAUGGGUU	1	0	0	1	1	0	3
Irf4	mmu-miR-125a-3p	mmu-mir-125a	ACAGGUGAGGUUCUUGGGAGCC	0	0	0	1	1	1	3
Irf4	mmu-miR-146b	mmu-mir-146b	UGAGAACUGAAUUCCAUAGGCU	1	0	0	1	1	0	3

Only binding sites of miRNA with SUM ≥ 3 shown.
Shaded area indicates overlapping binding sites of two distinct miRNAs

Supplemental Figure 1

E

Mouse Irf8 - 3'UTR

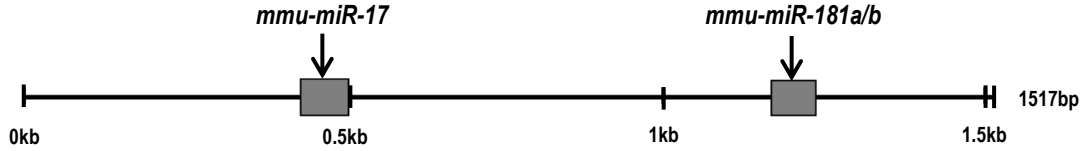

Gene	MicroRNA	StemLoop ID	Sequence (5′ → 3′)	miRWalk	miRanda	miRDB	PITA	RNA22	Targetscan	SUM
Irf8	mmu-miR-17	mmu-mir-17	CAAAGUGCUUACAGUGCAGGUAG	1	1	0	0	1	1	4
Irf8	mmu-miR-181b	mmu-mir-181b-2	AACAUUCAUUGCUGUCGGUGGGU	1	1	0	0	1	1	4
Irf8	mmu-miR-181a	mmu-mir-181a-1	AACAUUCAACGCUGUCGGUGAGU	1	1	0	0	0	1	3

Only binding sites of miRNA with SUM ≥ 3 shown

F

Mouse Id2 - 3'UTR

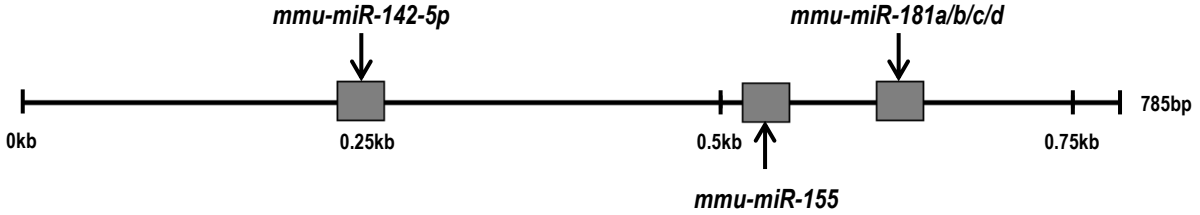

Gene	MicroRNA	StemLoop ID	Sequence (5′ → 3′)	miRWalk	miRanda	miRDB	PITA	RNA22	Targetscan	SUM
Id2	mmu-miR-181a	mmu-mir-181a-1	AACAUUCAACGCUGUCGGUGAGU	1	1	0	1	1	1	5
Id2	mmu-miR-181d	mmu-mir-181d	AACAUUCAUUGUUGUCGGUGGGU	1	1	0	1	1	1	5
Id2	mmu-miR-181b	mmu-mir-181b-2	AACAUUCAUUGCUGUCGGUGGGU	1	1	0	1	0	1	4
Id2	mmu-miR-181c	mmu-mir-181c	AACAUUCAACCUGUCGGUGAGU	1	1	1	0	0	1	4
Id2	mmu-miR-142-5p	mmu-mir-142	CAUAAAGUAGAAAGCACUACU	0	0	0	1	1	1	3
Id2	mmu-miR-155	mmu-mir-155	UUAAUGCUAAUUGUGAUAGGGGU	1	0	0	1	0	1	3

Only binding sites of miRNA with SUM ≥ 3 shown

G

Mouse SpiB - 3'UTR

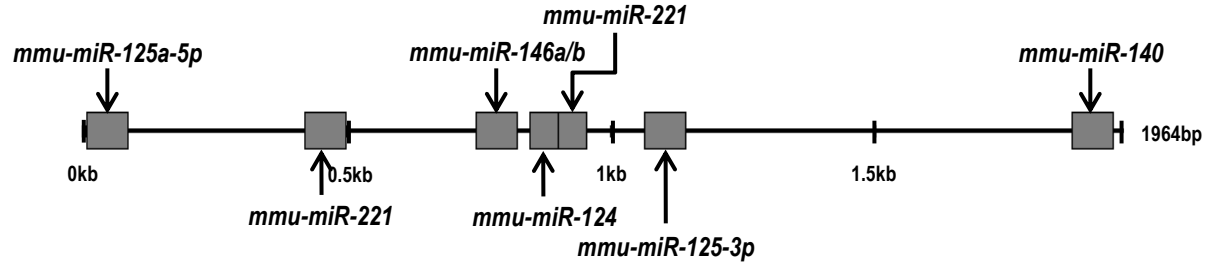

Gene	MicroRNA	StemLoop ID	Sequence (5′ → 3′)	miRWalk	miRanda	miRDB	PITA	RNA22	Targetscan	SUM
Spib	mmu-miR-221	mmu-mir-221	AGCUACAUUGUCUGCUGGGUUUC	1	1	0	1	1	1	5
Spib	mmu-miR-146b	mmu-mir-146b	UGAGAACUGAAUUCCAUAGGCU	1	1	0	1	0	1	4
Spib	mmu-miR-146a	mmu-mir-146a	UGAGAACUGAAUUCCAUGGGUU	1	1	0	1	0	1	4
Spib	mmu-miR-124	mmu-mir-124-2	UAAGGCACGCGGUGAAUGCC	1	1	0	1	0	1	4
Spib	mmu-miR-140	mmu-mir-140	CAGUGGUUUUACCCUAUGGUAG	0	0	0	1	1	1	3
Spib	mmu-miR-125a-3p	mmu-mir-125a	ACAGGUGAGGUUCUUGGGAGCC	1	0	0	1	1	0	3
Spib	mmu-miR-125a-5p	mmu-mir-125a	UCCCUGAGACCCUUUAACCUGUGA	1	0	0	1	1	0	3

Only binding sites of miRNA with SUM ≥ 3 shown

Supplemental Figure 1

H

Mouse Batf3 - 3'UTR

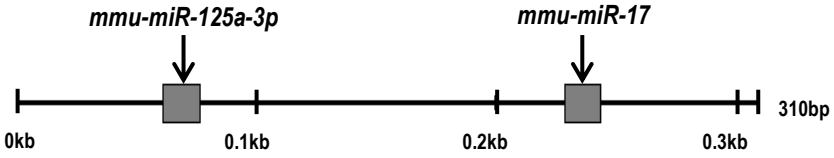

Gene	MicroRNA	StemLoop ID	Sequence (5′ → 3′)	miRWalk	miRanda	miRDB	PITA	RNA22	Targetscan	SUM
Batf3	mmu-miR-125a-3p	mmu-mir-125a	ACAGGUGAGGUUCUUGGGAGCC	1	1	0	1	1	0	4
Batf3	mmu-miR-17	mmu-mir-17	CAAAGUGCUUACAGUGCAGGUAG	1	1	0	1	1	0	4

Only binding sites of miRNA with SUM ≥ 3 shown

I

Mouse Notch2 - 3'UTR

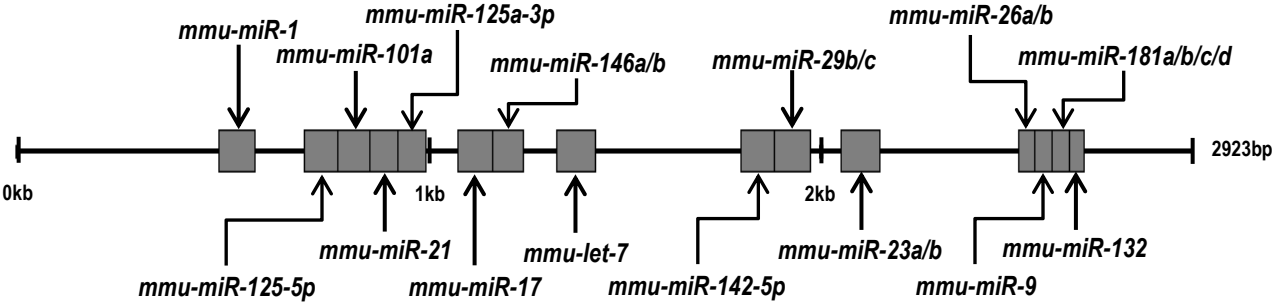

Gene	MicroRNA	StemLoop ID	Sequence (5′ → 3′)	miRWalk	miRanda	miRDB	PITA	RNA22	Target scan	SUM
Notch2	mmu-miR-9	mmu-mir-9-1	UCUUUGGUUAUCUAGCUGUAUGA	1	1	1	1	1	1	6
Notch2	mmu-miR-181c	mmu-mir-181c	AACAUUCAACCUGUCGGUGAGU	1	1	0	1	1	1	5
Notch2	mmu-miR-181a	mmu-mir-181a-1	AACAUUCAACGCUGUCGGUGAGU	1	1	0	1	1	1	5
Notch2	mmu-miR-21	mmu-mir-21a	UAGCUUAUCAGACUGAUGUUGA	1	1	0	1	1	1	5
Notch2	mmu-miR-142-5p	mmu-mir-142	CAUAAAGUAGAAAGCACUACU	1	1	0	1	1	1	5
Notch2	mmu-miR-125a-3p	mmu-mir-125a	ACAGGUGAGGUUCUUGGGAGCC	1	1	0	1	1	1	5
Notch2	mmu-let-7e	mmu-let-7e	UGAGGUAGGAGGUUGUAUAGUU	1	0	0	1	1	1	4
Notch2	mmu-miR-101a	mmu-mir-101a	UACAGUACUGUGAUAACUGAA	1	1	0	1	0	1	4
Notch2	mmu-let-7a	mmu-let-7a-1	UGAGGUAGUAGGUUGUAUAGUU	1	0	0	1	1	1	4
Notch2	mmu-miR-132	mmu-mir-132	UAACAGUCUACAGCCAUGGUCG	1	1	0	1	0	1	4
Notch2	mmu-let-7f	mmu-let-7f-1	UGAGGUAGUAGAUUGUAUAGUU	1	0	0	1	1	1	4
Notch2	mmu-miR-1	mmu-mir-1a-1	UGGAAUGUAAAGAAGUAUGUAU	1	1	0	1	0	1	4
Notch2	mmu-let-7b	mmu-let-7b	UGAGGUAGUAGGUUGUGUGGUU	1	0	0	1	1	1	4
Notch2	mmu-miR-26a	mmu-mir-26a-1	UUCAAGUAAUCCAGGAUAGGCU	1	0	0	1	1	1	4
Notch2	mmu-let-7g	mmu-let-7g	UGAGGUAGUAGUUUGUACAGUU	1	0	0	1	1	1	4
Notch2	mmu-miR-146a	mmu-mir-146a	UGAGAACUGAAUUCCAUGGGUU	1	0	0	1	1	1	4
Notch2	mmu-let-7c	mmu-let-7c	UGAGGUAGUAGGUUGUAUGGUU	1	0	0	1	1	1	4
Notch2	mmu-miR-181b	mmu-mir-181b-1	AACAUUCAUUGCUGUCGGUGGGU	0	1	0	1	1	1	4
Notch2	mmu-let-7i	mmu-let-7i	UGAGGUAGUAGUUUGUGCUGUU	1	0	0	1	1	1	4
Notch2	mmu-let-7d	mmu-let-7d	CUAUACGACCUGCUGCCUUUCU	0	0	0	1	1	1	3
Notch2	mmu-miR-181d	mmu-mir-181d	AACAUUCAUUGUUGUCGGUGGGU	0	1	0	1	0	1	3
Notch2	mmu-miR-17	mmu-mir-17	CAAAGUGCUUACAGUGCAGGUAG	1	0	0	1	1	0	3
Notch2	mmu-miR-23a	mmu-mir-23a	AUCACAUUGCCAGGGAUUUCC	0	0	0	1	1	1	3
Notch2	mmu-miR-29b	mmu-mir-29b-2	CUGGUUUCACAUGGUGGCUUAGAUU	1	0	0	1	1	0	3
Notch2	mmu-miR-23b	mmu-mir-23b	AUCACAUUGCCAGGGAUUACC	0	0	0	1	1	1	3
Notch2	mmu-miR-26b	mmu-mir-26b	UUCAAGUAAUUCAGGAUAGGU	1	0	0	1	0	1	3
Notch2	mmu-miR-29c	mmu-mir-29c	UAGCACCAUUUGAAAUCGGUUA	1	0	0	1	1	0	3
Notch2	mmu-miR-146b	mmu-mir-146b	UGAGAACUGAAUUCCAUAGGCU	1	0	0	1	0	1	3
Notch2	mmu-miR-125a-5p	mmu-mir-125a	UCCCUGAGACCCUUUAACCUGUGA	1	0	0	1	1	0	3

Only binding sites of miRNA with SUM ≥ 3 shown

Supplemental Figure 1

J

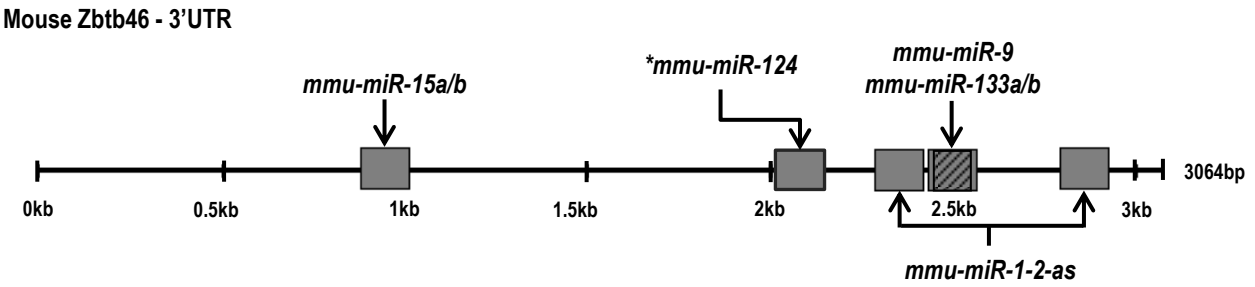

Gene	MicroRNA	StemLoop ID	Sequence (5′ → 3′)	miRWalk	miRanda	miRDB	RNA22	Targetscan	SUM
Zbtb46	mmu-miR-9	mmu-mir-9-1	UCUUUGGUUAUCUAGCUGUAUGA	1	1	0	1	1	4
Zbtb46	mmu-miR-1-2-as	mmu-mir-1-2-as	UACAUACUUCUUUACAUUCCA	1	1	0	1	1	4
Zbtb46	mmu-miR-133b	mmu-mir-133b	UUUGGUCCCCUUCAACCAGCUA	1	0	0	1	1	3
Zbtb46	mmu-miR-15a	mmu-miR-15a	UAGCAGCACAUAAUGGUUUGUG	1	0	0	1	1	3
Zbtb46	mmu-miR-15b	mmu-miR-15b	UAGCAGCACAUCAUGGUUUACA	1	0	0	1	1	3
Zbtb46	mmu-miR-133a	mmu-mir-133a-2	UUUGGUCCCCUUCAACCAGCUG	1	0	0	1	1	3

PITA omitted because Zbtb46 not registered
Only binding sites of miRNA with SUM ≥ 3 shown
Shaded area indicates overlapping binding sites of two distinct miRNAs
****mmu-miR-124 not in chart because SUM = 1***

Supplemental Figure 1. Identification of candidate miRNAs that potentially target the transcript of transcription factors in DC development. miRWalk2.0 was used to identify miRNAs with high probability to bind to the 3'UTR of the listed transcription factors. miRanda, miRWalk, miRDB, PITA, RNA22, and TargetScan prediction algorithms were used and miRNAs with significant scores from at least 3 of the algorithms were listed (SUM ≥ 3). (A) Candidate list of miRNAs that target TCF4 and the map of 3'UTR diagram for TCF4 with the predicted binding sites of the candidates. The same is shown for (B) Bcl6, (C) Irf2, (D) Irf4, (E) Irf8, (F) Id2, (G) SpiB, (H) Batf3, (I) Notch2, and (J) Zbtb46.